

Experimental study of the mutual influence of fibre Faraday elements in a spun-fibre interferometer

V.P. Gubin, S.K. Morshnev, Ya.V. Przhiyalkovsky, N.I. Starostin, A.I. Sazonov

Abstract. An all-spun-fibre linear reflective interferometer with two linked Faraday fibre coils is studied. It is found experimentally that there is mutual influence of Faraday fibre coils in this interferometer. It manifests itself as an additional phase shift of the interferometer response, which depends on the circular birefringence induced by the Faraday effect in both coils. In addition, the interferometer contrast and magneto-optical sensitivity of one of the coils change. A probable physical mechanism of the discovered effect is the distributed coupling of orthogonal polarised waves in the fibre medium, which is caused by fibre bend in the coil.

Keywords: Faraday effect, spun fibre, linear interferometer.

1. Introduction

We investigated an effect in a fibre-optic current sensor based on the Faraday effect and having two sensing elements in a highly birefringent spun-fibre linear reflective interferometer [1]. The Faraday effect is the occurrence of circular birefringence in an optical fibre placed in a longitudinal magnetic field. As a result, orthogonal circularly polarised light waves propagate in this fibre with different velocities, and a phase difference φ_F (Faraday phase shift), proportional to the magnetic field (current), is accumulated between them. An optical interferometer used to measure a phase shift contains generally two elements: a phase-shifting device (modulator) and a sensitive coil [2]. An interferometer scheme was proposed in [1], where both elements were made of magnetosensitive (spun) fibre and linked by the same fibre. It was suggested that mutual influence of these two fibre Faraday elements of the interferometer may occur in the aforementioned scheme. This suggestion was confirmed experimentally. The effect discovered may manifest itself as a nonlinearity of the output current sensor characteristic. The purpose of our study was to investigate experimentally this effect.

2. Experimental setup

To analyse experimentally the mutual influence of Faraday elements, we developed a linear reflective interferometer, a

V.P. Gubin, S.K. Morshnev, Ya.V. Przhiyalkovsky, N.I. Starostin, A.I. Sazonov V.A. Kotelnikov Institute of Radio Engineering and Electronics, Fryazino Branch, Russian Academy of Sciences, pl. Vvedenskogo 1, 141190 Fryazino, Moscow region, Russia; Profotek CJSC, Vereiskaya ul. 17, 121357 Moscow, Russia; e-mail: yankus.p@gmail.com, nis229@ire216.msk.su

Received 27 May 2014; revision received 4 August 2014
Kvantovaya Elektronika 45 (8) 754–758 (2015)
Translated by Yu.P. Sin'kov

schematic of which is presented in Fig. 1. Reflected light was recorded at the output of coupler (2) by photodiode (9). The voltage at the photodiode output was measured by a digital voltmeter.

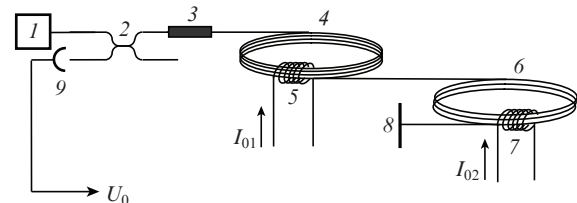


Figure 1. Schematic of the experimental setup: (1) radiation source; (2) directed coupler; (3) polariser; (4) modulator coil (first rotator); (5, 7) solenoids; (6) sensitive coil (second rotator); (8) mirror; (9) photodiode; I_{01} and I_{02} are currents.

A specific feature of this interferometer is that it is made entirely of magnetosensitive spun fibre and contains Faraday fibre elements (Faraday rotators) in a common fibre channel. The first element implements a dynamic or static phase shift, and the second is a sensitive coil (in a current sensor). For brevity, we will refer to them as the first and second Faraday rotators, respectively. The interferometer contains also a polariser and a mirror. Two orthogonal polarised light waves propagate in the interferometer; generally, their polarisation states (PSs) are elliptical [3–6]. In the absence of a magnetic field in rotators, the interferometer has a zero path difference for the circular components of orthogonal wave polarisations (i.e., it is a mutual device), because, when reflecting from the mirror, circularly polarised wave components change to orthogonal: the right-handed polarisation becomes a left-handed one and vice versa; as a result, both waves will have identical phase delays after a round trip. Due to the Faraday effect, a magnetic field introduces an uncompensated phase shift φ_F between the waves; hence, the radiation at the interferometer output will be linearly polarised with rotation of the plane of polarisation by $\varphi_F/2$. An analysis of the light intensity at the photodiode input allows one to calculate the desired phase shift φ_F , which is proportional to the magnetic field (and, correspondingly, current).

The light source was an erbium-doped fibre emitter with a wavelength of 1.55 μm , output power of 30 mW, and radiation spectrum 25 nm wide.

The interferometer elements (fibre coils and link) were made of conventional spun fibre with a beat length of built-in linear birefringence $L_b = 8$ mm and a spin pitch of birefrin-

gence axes $L_{\text{tw}} = 3$ mm. The spun fibre of rotators was wound on quartz tubes with a diameter $D = 20$ mm and length 100 mm. A longitudinal magnetic field in a fibre rotator was formed by a toroidal copper wire solenoid, the turns of which passed through the internal hole of a quartz tube and covered it outside. The first rotator contained $N_{11} = 9000$ fibre turns and $N_{12} = 50$ copper wire turns; the corresponding parameters of the second rotator were $N_{21} = 4484$ turns and $N_{22} = 60$ turns.

3. Experimental

The dc voltage component U_0 at the photodiode output can be presented as a function of currents in rotator solenoids by the relation

$$U_0 = U_{00}[1 + K_n \cos(\varphi_{F1} + \varphi_{F2} + \Delta\varphi_n)], \quad n = 1, 2, \quad (1)$$

$$\varphi_{F1} = a_1 I_{01} = 4VS_1 N_{11} N_{12} I_{01}, \quad (1a)$$

$$\varphi_{F2} = a_2 I_{02} = 4VS_2 N_{21} N_{22} I_{02}. \quad (1b)$$

Here U_{00} is the average voltage at the photodiode output; K_n is the interferometer contrast (visibility); φ_{F1} and φ_{F2} are the phase shifts in the first and second rotators, respectively; I_{01} and I_{02} are the currents in the solenoids of the first and the second rotator; $V \approx 7 \times 10^{-7}$ rad A^{-1} is the Verdet constant for quartz fibre; and S_1 and S_2 are the relative magneto-optical sensitivities of spun-fibre in the first and second rotators with respect to an ideal fibre. The $\Delta\varphi_n$ value is a constant phase additive, which was revealed in this study. Relation (1) is the output characteristic (response) of a linear reflective interferometer with two rotators. The subscripts $n = 1$ or 2 correspond to the output characteristic when the independent variable is the current in the first or second rotator, respectively.

Relation (1) was used to estimate the distortion of the interferometer characteristic caused by the mutual influence of rotators. This characteristic is determined below by the parameters U_{00} , K_n , S_1 , S_2 and $\Delta\varphi_n$.

We measured the output characteristics $U_0(I_{01})$ at $I_{02} = \text{const}$ and $U_0(I_{02})$ at $I_{01} = \text{const}$. Figure 2 shows the dependences $U_0(I_{01})$ for the first rotator, measured at two values of dc current I_{02} in the second rotator. The processing of measured data implied determination of the parameters using neighbouring extrema in the characteristic and fitting by the least-squares method. For example, one can measure accurately currents $I_{01\text{max}}$ and $I_{01\text{min}}$ in the extrema of the characteristic $U_0(I_{01})$ at $I_{02} = \text{const}$, i.e., for $\cos(\varphi_{F1} + \varphi_{F2} + \Delta\varphi_1) = 1$ and $\cos(\varphi_{F1} + \varphi_{F2} + \Delta\varphi_1) = -1$, respectively (see Fig. 2). Then, using the relation

$$\varphi_{F1} + \varphi_{F2} + \Delta\varphi_1 = 0, \quad (2)$$

one can determine the additive

$$\Delta\varphi_1 = -(\varphi_{F1} + \varphi_{F2}) = -(a_1 I_{01\text{max}} + a_2 I_{02}). \quad (3)$$

The same measurements yield

$$S_1 = \frac{\pi}{4VN_{11}N_{21}(|I_{01\text{max}} - I_{01\text{min}}|)}, \quad (4)$$

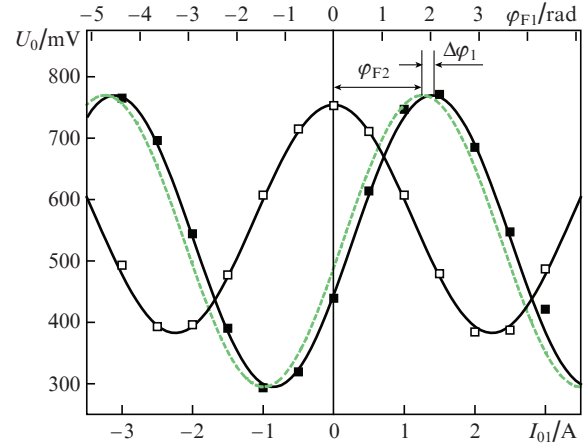


Figure 2. Interferometer output characteristics measured with a change in the current in the first rotator; the current in the second rotator is $I_{02} = (\square) 0$ and $(\blacksquare) -2$ A.

$$K_1 = \frac{U_{01\text{max}} - U_{01\text{min}}}{U_{01\text{max}} + U_{01\text{min}}}, \quad (5)$$

where $U_{01\text{max}}$ and $U_{01\text{min}}$ are the values of the characteristic in extrema. These parameters were determined more exactly by fitting relation (1) to experimental points of the entire measured characteristic using the least-squares method.

The solid curves in Fig. 2 is the result of a calculation based on relation (1). The parameters U_{00} , K_1 , S_1 and S_2 for these curves were determined using the aforementioned technique; note that $S_1 = 1.109$ and $S_2 = 1.164$ for $I_{02} = -2$ A and $S_1 = 1.112$ for $I_{02} = 0$. Two values are indicated for $\Delta\varphi_1$: the dashed line is the result of calculation for a current $I_{02} = -2$ A at $\Delta\varphi_1 = 0$, and the solid line is the result of calculation at $\Delta\varphi_1 = -0.195$ rad. It follows from Fig. 2 that, at $I_{02} = -2$ A, the experimental data correspond to the values calculated at $\Delta\varphi_1 = -0.195$ rad. In addition, Fig. 2 demonstrates that the interferometer contrast significantly increases in the presence of current in the second rotator.

A similar procedure was performed when measuring the characteristic of the second rotator: $U_0(I_{02})$ at $I_{01} = \text{const}$.

4. Results and discussion

Figure 3 shows the dependences of the phase additive $\Delta\varphi_1$ and contrast K_1 of the first rotator on the current I_{02} in the second rotator, and Fig. 4 presents the dependences of the phase additive $\Delta\varphi_2$ and contrast K_2 of the second rotator on the current I_{01} in the first rotator.

Figure 5 shows the dependences of the relative magneto-optical sensitivity S of one rotator on the phase shift φ_F in the other rotator.

The experimental data indicate the existence of a new physical effect – mutual influence of coils – in an interferometer with two Faraday fibre coils. We should note that the observed regularities are not caused by technical imperfections of the experimental setup, in particular, stray magnetic fields of the solenoids, heating of coils by currents through these solenoids, etc. Experiments were performed with differently arranged (spaced by a distance from 10 cm to 2 m) and oriented coils. Generally, the temperature of coil spun fibre affects the magneto-optical sensitivity; however, this influence was insignificant because of weak heating (few kelvins).

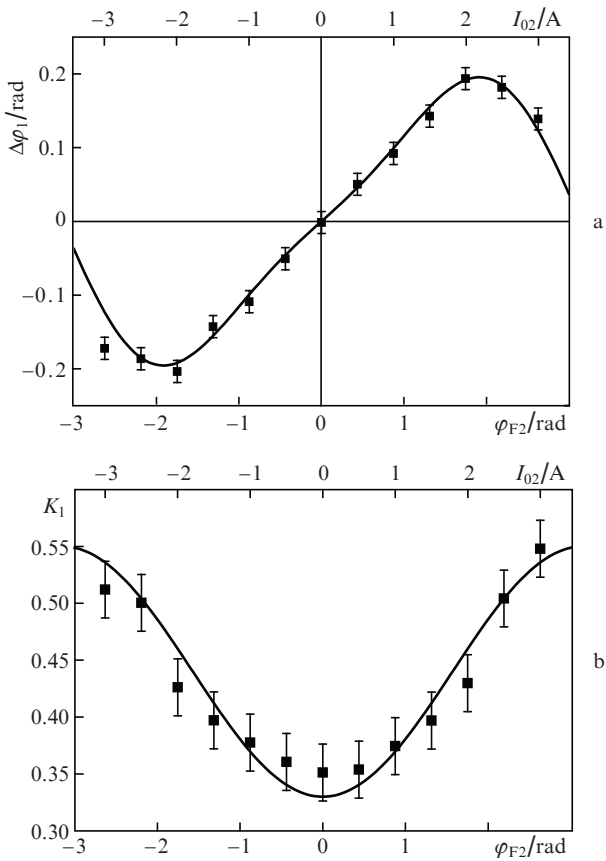


Figure 3. Dependences of the (a) phase additive and (b) contrast of the first-rotator characteristic on the current in the second rotator.

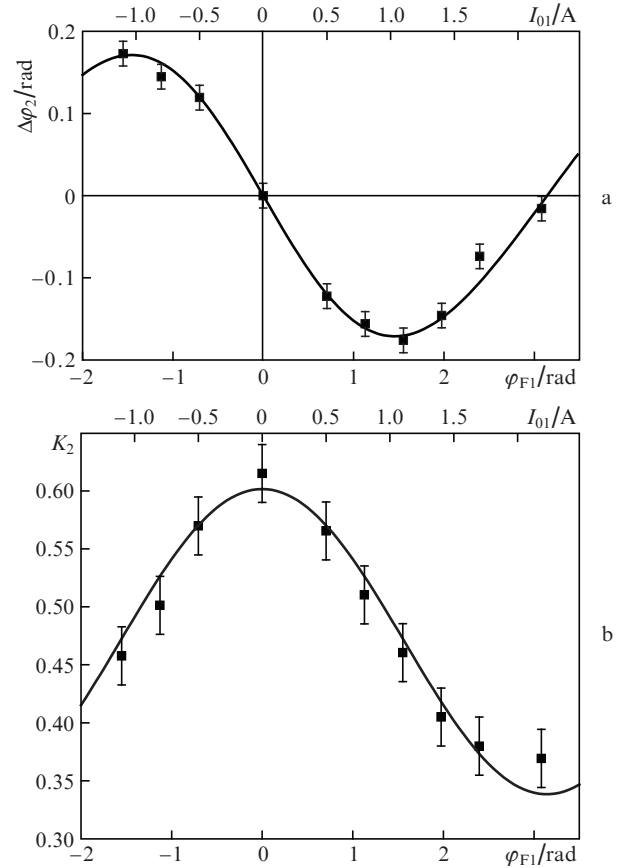


Figure 4. Dependences of the (a) phase additive and (b) contrast of the second-rotator characteristic on the current in the first rotator.

An analysis of the above-mentioned factors did not reveal their contribution to our experimental results. The latter can be formulated as follows. First, this is the occurrence of a phase additive to the interferometer current characteristic, measured in one rotator, in the presence of a dc magnetic field (current) in the other rotator. The additive sign depends on the current direction, and its value is a function of the current. The second result is the change in the contrast interferometer (visibility). In addition, there is a small change in the magneto-optical sensitivity of one of the fibre rotators (specifically, the first one) of the interferometer.

Thus, the characteristic of one of the rotators [for example, the first one, $U_0(\varphi_{F1})$] shifts along the abscissa axis not only by the value of the Faraday shift φ_{F2} in the second rotator but also undergoes an additional phase shift $\Delta\varphi_1$ (see Fig. 2). A similar phase shift, $\Delta\varphi_2$, but of opposite sign is observed in the characteristic $U_0(\varphi_{F2})$ at a constant shift φ_{F1} in the first rotator. It should be emphasised that a necessary condition for the occurrence of a phase additive is the presence of circular birefringence due to the Faraday effect in both rotators.

The phase additive is calculated by fitting the calculation parameters of relation (1) and the interferometer characteristic, which is measured experimentally. It is important to know the exact values of magneto-optical sensitivity of the rotators in the entire range of currents. The dependences $S_1(\varphi_{F2})$ and $S_2(\varphi_{F1})$ presented in Fig. 5 were calculated from relation (4) based on the spacing between the neighbouring extrema in the measured characteristic. It can be seen that mean sensitivities of the first and second rotators in the range of operating cur-

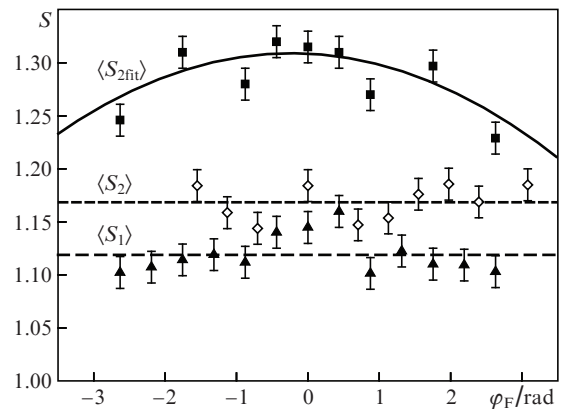


Figure 5. Dependences (▲) $S_1(\varphi_{F2})$ [calculation from formula (4)], (◇) $S_2(\varphi_{F1})$ [calculation from a formula similar to (4)], and (■) $S_{2fit}(\varphi_{F1})$ [calculation from formula (2) in the absence of phase additive ($\Delta\varphi_1 = 0$)].

rents (Faraday phase shifts) differ: $\langle S_1 \rangle = 1.119$ and $\langle S_2 \rangle = 1.168$; this difference slightly exceeds the measurement error (1%–2%). We did not analyse the nature of this discrepancy. Figure 5 shows also that the S_2 value is independent (within the measurement error) of the circular birefringence in the first rotator. The mean S_2 value almost coincides with the value at zero current ($S_2 = 1.164$). At the same time, S_1 slightly decreases with an increase in the modulus of φ_{F2} . We relate the existence of the dependence $S_1(\varphi_{F2})$ to the mutual influence of rotators.

Table 1. Dependence of the additive g on the second-rotator parameters for different interferometer designs (Nos 1–3).

No	Fibre	L_b /mm	L_{tw} /mm	Influence of bending	D_2 /mm	σ	S_2	$\varphi_{F1}(I_{01max})$ /rad	$\Delta\varphi_1$ /rad	g
1	Conventional	8	3	Strong	14	0.19	0.9385	0.90	0.121 ± 0.015	0.134
2	Conventional	8	3	Intermediate (this study)	20	0.19	1.164	0.88	0.092 ± 0.015	0.105
3	Microstructured	5	3.5	Weak	20	0.35	0.97	0.88	0.062 ± 0.01	0.071

Note: $D_{1,2}$ are the bend diameters of fibre rotators; $D_1 = 20$ mm.

Note that good agreement between the calculation and experiment can also be obtained at a zero phase additive by fitting the S_2 value in the calculation; the latter, generally speaking, may change because of the mutual influence of the rotators. However, the dependence $S_{2fit}(\varphi_{F1})$ obtained by this fitting (Fig. 5) yields a significantly overestimated sensitivity, especially at small φ_{F1} values. For example, at small currents, $S_{2fit} \approx 1.3$, a value inconsistent with $S_2 = 1.164$, measured at a zero current in the first rotator. Therefore, we consider unrealistic the absence of the phase additive. We should emphasise that, according to our experiments, the S_2 value can be assumed constant.

Note that the S_1 and S_2 values turned out to be larger than unity in our measurements. We explain this fact by the difference between the Verdet constant in spun fibre in use from the value of this constant for pure quartz, which was applied in the calculations.

The phase additive in one of the rotators depends periodically on the circular birefringence in the other rotator. The approximated dependences $\Delta\varphi_1 = 0.18\sin(\varphi_{F2}) - 0.04\sin(2\varphi_{F2})$ and $\Delta\varphi_2 = -0.17\sin(\varphi_{F1}) - 0.01\sin(2\varphi_{F1})$ in Figs 3a and 4a are in satisfactory agreement with the experiment.

The dependence of the interferometer contrast on the circular birefringence in one of the rotators is also periodic; it can adequately be approximated by a cosine function of the Faraday phase shift (Figs 3b, 4b): $K_1 = 0.47[1 - 0.28\cos(\varphi_{F2})]$ and $K_2 = 0.48[(1 + 0.25\cos(\varphi_{F1}))]$.

Thus, mutual influence of fibre Faraday coils (rotators) in the common channel of the spun-fibre interferometer was experimentally revealed. A mathematical model of this effect has not yet been developed. It can be explained as follows. The rotators in the scheme under consideration operate under different conditions. In the second rotator, the forward and backward light waves do not pass through the medium of the first rotator when interacting with 'their' magnetic field. At the same time, in the first rotator, the forward wave passes through the medium of the second rotator after the interaction with its magnetic field, while the backward wave passes through it before the beginning of this interaction. Circular birefringence is induced in the medium of the second rotator due to the nonreciprocal Faraday effect. We believe that the phase additive is due to the fibre bend in the coil winding. Each wave in a bent fibre is a superposition of orthogonally polarised coupled waves. This coupling, being distributed over fibre, may change the initially accumulated phase of each wave passing through the medium with 'nonreciprocal' circular birefringence, i.e., induce a phase additive in the first rotator. Since birefringence is due to the nonreciprocal Faraday effect, the additionally accumulated wave phase is not compensated for during the round trip in the interferometer. Note that the wave coupling caused by bending should depend on the degree of anisotropy of spun fibre, which is characterised by the parameter $\sigma = L_{tw}/2L_b$ [6].

Concerning the formation of a phase additive in the second rotator, it may be due to the occurrence of a phase additive in the first rotator, induced, as was said above, by the presence of birefringence in the second rotator.

We also suggest that the aforementioned coupling of orthogonally polarised waves, induced by bending, leads to redistribution of the initial wave power into the 'coherent' and 'incoherent' channels (optical paths) of the interferometer [7] and thus changes the contrast.

To confirm the above hypothesis, we measured the relative additives $g = \Delta\varphi_1/\varphi_{F1}(I_{01max})$ for three interferometer designs. The results are listed in Table 1. It can be seen that a decrease in the fibre bend radius D_2 leads to an increase in the phase additive $\Delta\varphi_1$ (or g). In addition, a rise in the built-in birefringence (decrease in L_b , increase in σ) increases the spun fibre resistance to bending [8, 9] and, as a consequence, reduces the phase additive $\Delta\varphi_1$, which is confirmed by the reduction of the relative phase additive g .

The effect discovered may cause nonlinearity of the output characteristic of a current sensor based on the interferometer under consideration.

5. Conclusions

It was found experimentally that an all-fibre linear reflective interferometer containing two Faraday fibre coils and a link in-between, made of spun fibre, exhibits mutual influence of coils: there is an additional phase shift (phase additive) of the output characteristic (response) of the interferometer, which depends on the circular birefringence in both coils. The interferometer contrast and the magneto-optical sensitivity of one of the coils change as well. The phase additive decreases with increasing built-in linear birefringence of spun fibre and/or with increasing coil winding radius. The discovered effect can be caused by the distributed coupling of orthogonal polarised waves in the fibre medium, which is caused by fibre bending. This effect may lead to nonlinearity of the output characteristic of a current sensor based on the above-considered interferometer. To minimise the consequences of this effect in a current sensor with a small sensitive coil, one should apply spun fibre with high built-in birefringence, e.g., microstructured spun fibre.

References

1. Starostin N.I., Chamorovsky Yu.K., Ryabko M.V., et al. *Foton-Ekspress*, No. 6 (94), 38 (2011).
2. Frosio G., Dancliker R. *Appl. Opt.*, **33**, 6111 (1994).
3. Laming R.I., Payne D.N. *J. Lightwave Technol.*, **7** (12), 2084 (1989).
4. Gubin V.P., Isaev V.A., Morshnev S.K., et al. *Kvantovaya Elektron.*, **36** (2), 287 (2006) [*Quantum Electron.*, **36** (2), 287 (2006)].
5. Michie A., Canning J., Bassett I., et al. *Opt. Express*, **15**, 1811 (2007).

6. Przhiyalkovsky Ya.V., Morshnev S.K., Starostin N.I., Gubin V.P. *Kvantovaya Elektron.*, **43** (2), 167 (2013) [*Quantum Electron.*, **43** (2), 167 (2013)].
7. Gubin V.P., Morshnev S.K., Starostin N.I., et al. *Kvantovaya Elektron.*, **41** (9), 815 (2011) [*Quantum Electron.*, **41** (9), 815 (2011)].
8. Chamorovsky Yu.K., Starostin N.I., Ryabko M.V., et al. *Opt. Commun.*, **282**, 4618 (2009).
9. Chamorovsky Yu.K., Starostin N.I., Morshnev S.K., et al. *Kvantovaya Elektron.*, **39** (11), 1074 (2009) [*Quantum Electron.*, **39** (11), 1074 (2009)].